

Recent advances in high-resolution MEMS DM fabrication and integration

Thomas Bifano¹

Boston University

Steven Cornelissen

Boston Micromachines Corporation

Paul Bierden

Boston Micromachines Corporation

ABSTRACT

Deformable mirrors fabricated using microelectromechanical systems technology (MEMS-DMs) have been studied at Boston University (BU) and developed/commercialized by Boston Micromachines Corporation (BMC) over the past decade. Recent advances that might have an impact on surveillance telescopes include demonstration of 4092 actuator DMs with continuous mirror face-sheets, and segmented DMs capable of frame rates of greater than 20kHz for devices with up to 1020 independent segments.

The 4092 actuator DM, developed by BMC for the Gemini Planet Imaging GPI instrument, was recently delivered to the GPI instrument development team. Its packaging and platform development are described, and the performance results for the latest prototype devices are presented.

1. INTRODUCTION

We have designed, fabricated, and tested a variety deformable mirrors (DMs) for adaptive optics (AO) over the past decade. These DMs could substantially extend the scientific capabilities of ground and space-based astronomical telescopes.

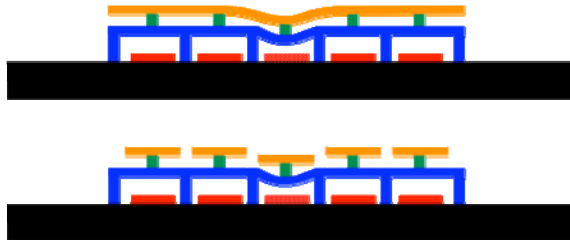


Fig. 1: Schematic cross section of continuous and segmented BU MEMS DMs. The mirror is connected by posts to an array of electrostatic actuators. Actuator deflection is approximately proportional to the square of voltage applied to the rigid electrodes on the wafer substrate. Top: continuous mirror DM. Bottom: segmented mirror DM.

The DMs are fabricated using silicon microelectromechanical (MEMS) production techniques, in which thin films of silicon and sacrificial material are alternately deposited, lithographically patterned, and etched to produce an integrated electromechanical system. The DM architecture is based on a scalable array of parallel plate electrostatic actuators, fabricated in silicon through semiconductor batch processing. Each square actuator plate is rigidly connected to the silicon substrate along two of its edges, and is suspended above an addressable electrode. Voltage applied to that electrode imposes an electrostatic attractive force on the electrically grounded actuator plate, causing it to bend toward the substrate in proportion to the square of applied voltage. Each actuator plate has a central post connected to a continuous or segmented mirror layer (Fig. 1).

The family of innovative products that we have produced, in continuous collaboration with academic researchers and students from BU, share a heritage in the original design and manufacturing approach used. These products now include mirrors with 32 to 4092 actuators, mirror apertures from 1.5mm to 26mm, and stroke from 2 μ m to 8 μ m.

¹ Address correspondence to Thomas Bifano, Photonics Center, 8 Saint Mary's Street, Boston, MA 02215, 617-314-4083, tgb@bu.edu

BMC products in widespread use include the MultiDM, with 140 actuators and a USB controlled driver, and the KiloDM and KiloSLM, continuous and segmented versions of a 1020 actuator device that features 20kHz frame rate. BMC also produces drivers and software for DMs and has custom-made several unique DMs for the astronomical imaging community.

A principal application for these DMs are high-resolution, high-contrast astronomical telescope compensation with AO. Open-loop, precise, and high-resolution control, is possible uniquely with MEMS-DM, and is indispensable for the next generation of telescope instruments.

The design and manufacturing approaches developed in our MEMS DM research offer inherent advantages over alternative approaches:

Design

- The device is scalable: increasing the size of the DM and its spatial resolution is achieved simply by adding identical actuators to the array (i.e. by copying and pasting lithographic mask features).
- The device is mechanically stiff and has low mass, allowing control bandwidths of tens of kilohertz.
- The actuation mechanism is repeatable to sub-nanometer precision, consumes almost no power, exhibits no hysteresis, and is unaffected by billions of cycles of operation.

Manufacturing

- The production approach does not call for exotic materials or tolerances: it can be made using a MEMS foundry and begins with an optically smooth, flat, and inexpensive substrate.
- Devices are batch produced twenty wafers at a time, so that while development costs are high, commercial production and replication costs are low.
- Hundreds of devices can be produced on each wafer, allowing broad parameter variation in a single batch production cycle. This accelerates research and prototyping.

MEMS-DM research offers the rare opportunity to introduce technology that is both more economical and more capable than the state-of-the-art. They reduce size, weight and power by considerably more than an order of magnitude, and are available commercially for a fraction of the cost of conventional DMs.

2. HIGH-RESOLUTION MEMS DM

A recent development project involved design, fabrication, and testing of a 4092 actuator continuous membrane DM and driver for the Gemini Planet Imaging system, building on the commercially successful and widely used BMC KiloDM device [1-3]. In the GPI instrument, the MEMS DM is used as a “tweeter” for high-spatial-resolution compensation of atmospheric turbulence, and a lower order macroscale piezoelectric DM is used as a woofer for lower-order compensation of turbulence, and to correct any static shape errors in the optical system. The core requirements for the MEMS DM are outlined in Table 1. This DM and driver are referred to as the “4K” throughout the remainder of this paper.

Table 1: 4K DM specifications

Description	Requirement
Actuators	4092
Stroke	3μm
Actuator pitch	400μm
Bandwidth	~2.5 kHz
Inter-actuator stroke	>1μm

The device was manufactured using a foundry MEMS process, and three independent batch processing runs were required to develop the process and achieve required mirror quality and actuator performance and yield.

Achieving a 100% actuator yield was the main challenge in this development effort due to the large size of the device and the limited number of devices processed in the three fabrication runs that were conducted. The low-order unpowered surface figure error of these large devices is mainly due to the bow in the silicon substrate on which the DM is fabricated resulting from mismatched film stresses on the front and back side of the silicon wafer. The resulting curvature leads to a peak-to-valley surface figure error of about $4\mu\text{m}$ in the active aperture. Although undesirable, most of this low-order error is spherical and astigmatic and may be removed using the woofer DM. The actuator yield loss has contributed to a handful of microscopic defects that were introduced during the fabrication process. Fig. 2 is an interferometric surface map of one of the finished, packaged, and coated 4K DMs, showing the device, an interferometric map of topography, and a map of anomalous actuator locations.

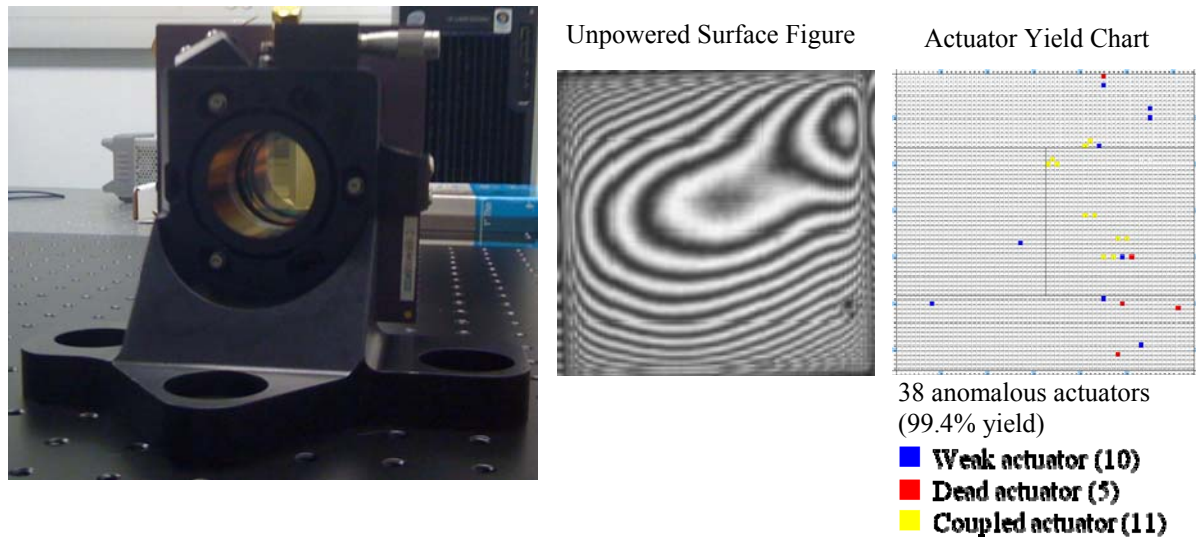


Fig. 2: 4092 actuator MEMS DM (Left); Typical unpowered surface figure of DM ($\sim 4\mu\text{m}$ P-V) (Center); Actuator yield chart of device showing 38 anomalous actuators (Right)

To evaluate the DM's ability to correct for the high-order wavefront aberrations expected at the Gemini Observatory, and to investigate the effects of the anomalous actuators, the DM was controlled to sample wavefront error maps. Since the woofer DM for the GPI instrument has sufficient stroke to compensate for both the low-order atmospheric aberrations and the unpowered surface figure of the DM, the shape of the DM was controlled to a shape in which the unpowered DM figure was added to the wavefront error map to represent the true shape that the DM must take to achieve the desired imaging quality. As shown in Figure 10, the DM was able to match this shape to less than 14nm rms with the 38 anomalous actuators (with these actuators masked out an error of less than 3nm rms was achieved – this is within the controller and measurement error of the closed-loop control system used for this experiment).

A modulator drive electronics system was developed for the 4K DM. This compact electronics unit uses high-density flex cables to carry the high-voltage drive signals to the DM. To keep the optical footprint of the DM small, a custom ceramic package was designed to which the DM die is mounted and wire bonded. High-density connectors for the 4K DM are attached directly to the back of the ceramic chip carrier (Fig. 4) so that the overall size of the package could remain small – $127\text{mm} \times 115\text{mm}$. These electronics can provide 14-bit resolution signals to the DM actuators to achieve sub-nanometer control. Low voltage frame signals are sent to the driver internal FPGA using a 200MB/s , 32-bit LVDS DIO card using a PC. Frame rates in excess of 20kHz , with a latency of $45\mu\text{s}$, can be achieved for a 4K DMs, but only for steps much smaller than the full-scale DM range. By reconfiguring the driver boards, a 1020 actuator DM can be driven at frame rates greater than 60kHz , with $15\mu\text{s}$ latency to enable high bandwidth AO controllers.

The drive electronics for a 4K DM operating at 10kHz consume approximately 120Watts of power. Most of this power is used to drive the high-voltage supplies and amplifiers, since the individual MEMS DM actuators consume only microwatts of power.

A new DM drive electronics architecture is currently under development that will reduce the total power consumption of the DM drive electronics by two orders of magnitude using multiplexing. These electronics will take advantage of the electrostatic actuator's ability to hold its charge to eliminate the need for a single DAC and amplifier for each DM actuator. These next generation electronics, intended for use in space-borne astronomical instruments where small size and low power consumption are very beneficial, will have 16-bit resolution with a goal of <10pm step control of the DM actuators.

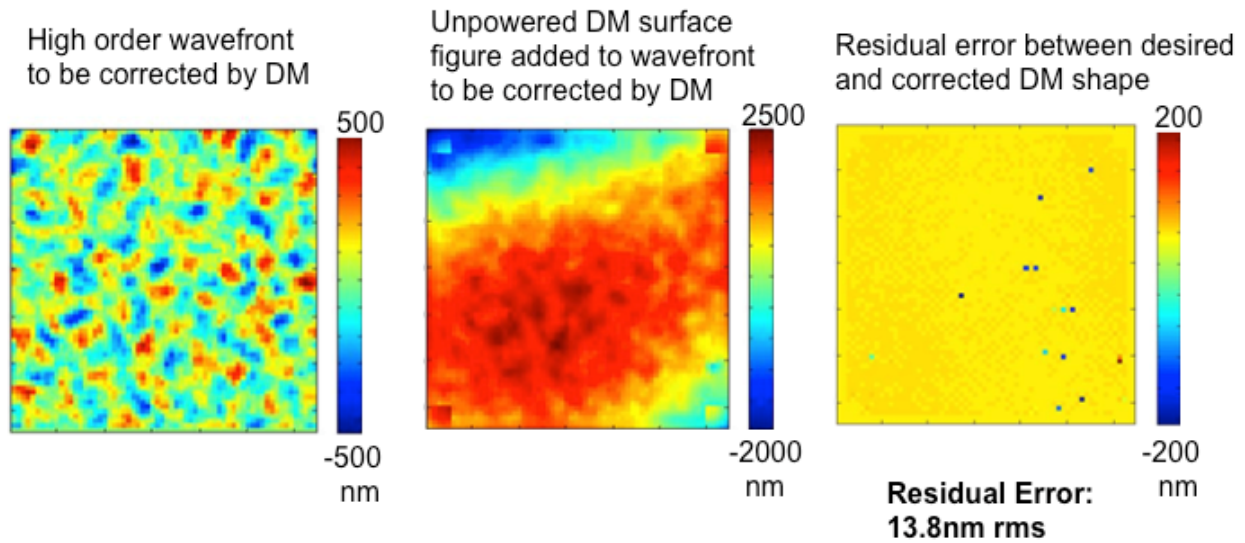


Fig 3 Residual wavefront error after 4K DM is controlled to a desired shape representative of the high-order atmospheric aberrations to be corrected by the tweeter DM is measured to be 13.8nm rms (right) with 38 anomalous actuators in the aperture. Left: The wavefront to be corrected for using the tweeter DM that remains after the woofer DM has compensated for the low-order errors, including the unpowered tweeter DM surface figure. Center: Actual shape tweeter DM must take to correct for wavefront error (unpowered DM shape added to wavefront error).

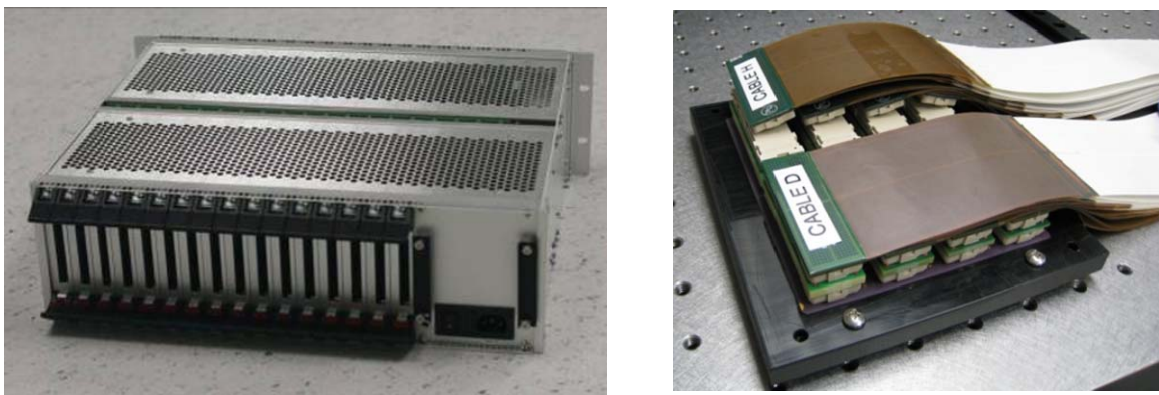


Fig. 4: 4K MEMS DM drive electronics unit (right) designed for the MEMS DMs. The modular design can be configured to drive DMs with 128-4092 actuators and can drive multiple DMs if needed. High-density flex cables connect directly to the back of the DM carrier to minimize its size (right)

3. HIGH-SPEED SEGMENTED DMs

In addition to continuous membrane DMs, BMC has also developed a family of segmented mirror DMs. BMC's. These have been used with parallel interferometric feedback sensors to steer and compensate beams propagating through turbulence in a number of prior studies for communications and targeting, at bandwidths of up to 1kHz in the field [4, 5]. Generally, the advantage of segmented DMs is that they can use phase wrapping to compensate wavefront errors with amplitudes larger than the DM actuator stroke.

Generally, these applications are highly constrained by size, weight, and power consumption of the AO system. MEMS DMs are promising because of their compact dimensions and low-power drivers, enabled by low capacitance (~100fF) electrostatic actuators. Overall, MEMS DMs reduce by more than an order of magnitude the volumetric size, total weight, and consumed power of in comparison to commercially available alternative DMs.

Over the past several years, experiments have been conducted at the Air Force's Atmospheric Simulation and Adaptive-optics Laboratory Testbed (ASALT), yielding comparisons among MEMS-based AO and conventional AO. Using the first generation of high-resolution MEMS DMs with 1020 active segments, researchers at ASALT concluded that implementation of a MEMS AO system would allow for observing at higher zenith angles (lower elevation angles) through deeper turbulence [6].

In some cases, it is desirable to increase the speed of wavefront control using segmented DMs to respond to applications for which the aberration time scales are as small as a few tens of microseconds, such as in boundary layer turbulence and jitter in beam propagation through an aircraft window.

The basic architecture of the MEMS DM actuator is relies on parallel electrostatic attraction between the fixed electrode and the compliant electrode. We can gain an understanding of its electromechanical behavior of the actuator by approximating the actuator as a fixed, planar lower electrode with length (and width) L and a compliant, planar upper electrode, separated by an initial gap g . If we apply a voltage V across the gap, the center of the compliant upper electrode deflects by an amount w . With these assumptions, the electrostatic attractive force is:

$$F_E = \frac{\epsilon L^2 V^2}{2(g-w)^2}$$

where ϵ is the permittivity of free space (8.8pF/m). Assuming the compliant actuator electrode acts as an elastic beam with fixed ends, the actuator mechanical force that resists this actuation is:

$$F_A = \frac{16Et^3w}{L^2}$$

where E is the elastic modulus of silicon (170GPa), t is the actuator plate thickness, and L is the actuator span. An equilibrium force balance yields:

$$V = \sqrt{\frac{32Et^3w(g-w)^2}{L^4\epsilon}}$$

The combined resonant frequency of an actuator and its mirror segment places one limit on the achievable update rate of the DM. To first order, that resonant frequency is simply the mechanical spring resonance of the compliant actuator and mirror segment. Spring resonance, in turn, can be approximated if the device's mechanical stiffness and effective mass are known. Specifically:

$$f_n = \frac{1}{2\pi} \sqrt{\frac{k}{m}} = \frac{1}{2\pi} \sqrt{\frac{(16Et^3/L^2)}{\rho L^2(t+t_m)}} = \frac{1}{2\pi L^2} \sqrt{\frac{(16Et^3)}{\rho(t+t_m)}}$$

where f_n is the resonant frequency, in hertz, k is the mechanical stiffness, m is the effective mass of the compliant actuator membrane and mirror segment, ρ is the density of silicon (2330kg/m³), and t_m is the thickness of the mirror segment.

It can be seen that the actuator span L has a strong effect on the natural frequency, making it possible to increase the potential speed of an actuator by reducing its mechanical span. Segment flexure can also affect dynamic performance. If the lowest resonant mode of the mirror segment, which is connected to the actuator membrane by a rigid central post, occurs at a frequency lower than the combined effective resonance previously calculated, then the mirror mode will dominate segment settling time. A fix for this is to stiffen the mirror segment. The frequency of the lowest flexural mode of the mirror will scale roughly in proportion to its thickness, t_m . Thickening the mirror can cause this mode to be much higher in frequency and lower in amplitude, reducing its impact on performance. The cost is a lower combined resonant frequency for the actuator-mirror system, scaling with the square root of t_m .

BMC has developed a prototype 1020 segment MEMS DM that takes advantage of our experience with electrostatic actuator dynamics and design. The goal was to improve dynamic performance of segmented DMs intended for use in high-speed applications. Results are illustrated in Fig. 5. The baseline DM (denoted “Baseline SLM” referring to its use as a reflective spatial light modulator) was a commercial BMC KiloDM similar to the one used recently [6] in the ASALT test bed and in technology demonstrations at LLNL for free-space laser propagation and for fast ignition fusion [4, 5]. The graph shows measured segment motion in response to step changes in actuator input voltage: from 0V to 150V, and then subsequently from 150V to 0V. For the baseline SLM, the initial displacement from rest position to a displacement of ~1200nm appears overdamped, settling to within 5% of the steady state position within ~50μs. After reaching steady state, the actuation step is reversed, and the actuator returns to its initial position within about 50μs. Note the presence of a faster dynamic response superimposed on the slower decay occurring immediately after this step change in input is applied. This is attributable to the combined effects of mirror flexure and squeeze-film stiffening.

The baseline DM device featured 300μm actuator pitch (~ L), and 3μm mirror segment thickness (t_m). A new device was designed with 250μm actuator pitch, along with proprietary geometric changes in actuator geometry to reduce the influence of squeeze-films on dynamic performance. The results were exceptional. In Fig. 5, the measured behavior of the “New SLM” is plotted in response to the same step functions in actuation input that were applied to the baseline device. It can be seen that the device settles to within 5% of its steady state value in ~15μs for both actuation directions – a threefold speed improvement.

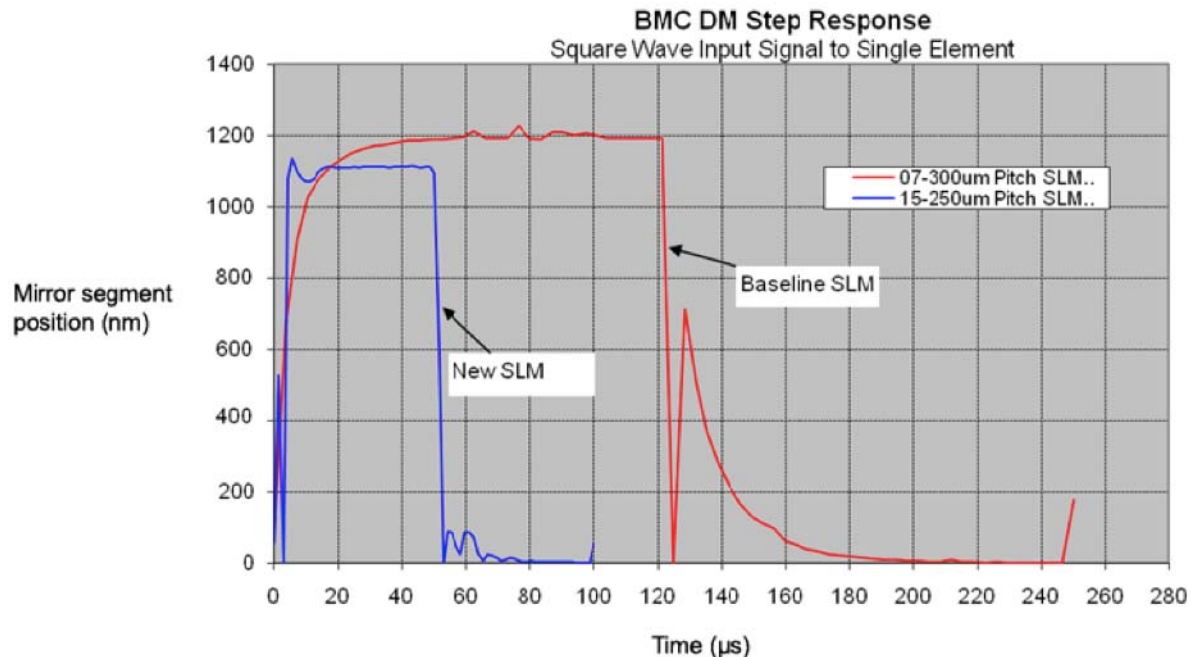


Fig. 5: Measured bi-directional step response for a single actuator-mirror segment in the baseline device and in a prototype new device optimized for speed. The setting time to within 5% of steady state for the baseline device is $\sim 50\mu\text{s}$, and for the new device is $\sim 15\mu\text{s}$. This improvement in speed can be exploited in innovative new AO control strategies.

4. CONCLUSIONS

BU and BMC have developed a number of high-resolution DMs in both continuous and segmented formats. These DMs now comprise a family of commercially available products, and the BU/BMC team has developed considerable experience in developing first-of-their-kind wavefront corrector technology prototypes (mirrors, packaging, and drivers). Recent advances in numbers-of-actuators in continuous membrane DMs, and dynamics of actuators in segmented mirror DMs have led to new capabilities that could be useful in future AO systems.

5. REFERENCES

- [1] Cornelissen SA, Bierden PA, Bifano TG, Lam CV, "4096-element continuous face-sheet MEMS deformable mirror for high-contrast imaging," *Journal of Micro/Nanolithography, MEMS and MOEMS*, [8], 031308-031308, (2009).
- [2] Macintosh B, Graham J, Palmer D, Doyon R, Gavel D, Larkin J, Oppenheimer B, Saddlemyer L, Wallace JK, Bauman B, Evans J, Erikson D, Morzinski K, Phillion D, Poyneer L, Sivaramakrishnan A, Soummer R, Thibault S, Veran J-P, "The Gemini Planet Imager," *Advances in Adaptive Optics II*, Orlando, FL, USA, *SPIE*, [6272], 62720L-62712, (2006).
- [3] Macintosh B, Graham J, Palmer D, Doyon R, Gavel D, Larkin J, Oppenheimer B, Saddlemyer L, Wallace JK, Bauman B, Erikson D, Poyneer L, Sivaramakrishnan A, Soummer R, Veran JP, "Adaptive optics for direct detection of extrasolar planets: the Gemini Planet Imager," *Comptes Rendus Physique*, [8], 365-373, (2007).
- [4] Baker K, Stappaerts E, Gavel D, Wilks S, Tucker J, Silva D, Olsen J, Olivier S, Young P, Kartz M, Flath L, Kruevivitch P, Crawford J, Azucena O, "High-speed horizontal-path atmospheric turbulence correction using a large actuator-number MEMS spatial light modulator in an interferometric phase conjugation engine," *Optics Letters*, [29], 1781-1783, (2004).

- [5] Baker KL, Stappaerts EA, Homoelle DC, Henesian MA, Bliss ES, Siders CW, Barty CPJ, “Interferometric adaptive optics for high-power laser pointing and wavefront control and phasing,” *Journal of Micro/Nanolithography, MEMS and MOEMS*, [8], 033040-033014, (2009).
- [6] Smith JC, Sanchez DJ, Oesch DW, Engstrom N, AgruelloLoretta, Tewksbury-Christle CM, Vitayaudom KP, Kelly PR, “Initial results from implementing and testing a MEMS adaptive optics system,” Bellingham, WA, , *Society of Photo-Optical Instrumentation Engineers*, [7466], 74660F-74661:74611, (2009).